Table 5 Comparison between the mean values of individual parameters in benign diseases and malignant diseases

	Benign ($n = 109$)	Malignant ($n = 106$)	p value
Age (mean ± SD)	69.2 ± 10.2	64.3 ± 11.8	0.001
Serum albumin (g/dl)	3.6 ± 0.7	3.4 ± 0.7	0.002
AST (IU/l)	276.9 ± 270.5	182.9 ± 199.5	0.004
ALT (IU/l)	207.4 ± 117.1	176.5 ± 248.4	0.296
T. bilirubin (mg/dl)	3.9 ± 3.7	5.7 ± 6.3	0.011
PT-INR >1.5 (yes/no)	10/99	8/98	0.807
Platelet count <100000/μl (yes/no)	19/90	13/93	0.340

Table 6 Results of univariate analysis with regard to hypoalbuminemia

	Serum albumin (g/dl)		p value	OR (95 % CI)
	≤2.8 ($n = 40$)	>2.8 ($n = 175$)		
Hypotension requiring dopamine ≥5 μl/kg per min or any dose of dobutamine (yes/no)	10/30	9/166	<0.001	6.148 (2.305–16.396)
Disturbance of consciousness (yes/no)	11/29	6/169	<0.001	10.684 (3.665–31.144)
PaO2/FiO2 ratio <300 (yes/no)	7/33	2/173	<0.001	18.348 (3.649–92.251)
Serum creatinine >2.0 mg/dl (yes/no)	2/38	2/173	0.158	4.553 (0.622–33.344)
PT-INR >1.5 (yes/no)	12/28	6/169	<0.001	12.071 (4.189–34.788)
Platelet count <100000/μl (yes/no)	16/24	16/159	<0.001	6.625 (2.932–14.969)
WBC count >12000 or <4000/μl (yes/no)	11/29	51/124	1.000	0.922 (0.428–1.985)
CRP ≥5 mg/dl (yes/no)	24/16	57/118	0.002	3.105 (1.531–6.298)
T-Bil ≥5 mg/dl (yes/no)	22/18	94/81	1.000	1.053 (0.528–2.100)
Body temperature >38 or <36 °C (yes/no)	21/19	69/106	0.156	1.698 (0.851–3.387)
Etiology (malignant/benign)	24/16	82/93	0.162	1.701 (0.846–3.422)
Age ≥75 years (yes/no)	10/30	47/128	1.000	0.908 (0.412–2.000)
Inpatient/Outpatient	25/15	79/96	0.055	2.025 (1.000–4.103)
Stent dysfunction (yes/no)	15/25	63/112	1.000	1.067 (0.524–2.171)
Death/alive	8/32	1/174	<0.001	43.500 (5.259–359.791)

Table 7 Results of univariate analysis with regard to mortality

Factor	Death ($n = 9$)	Alive ($n = 206$)	p value	OR (95 % CI)
Hypotension requiring dopamine ≥5 μl/kg per min or any dose of dobutamine (yes/no)	4/5	15/191	0.004	10.197 (2.474–41.972)
Disturbance of consciousness (yes/no)	5/4	12/194	<0.001	20.208 (4.796–85.145)
PaO_2/FiO_2 ratio <300 (yes/no)	3/6	6/200	0.004	16.667 (3.344–83.072)
Serum creatinine >2.0 mg/dl (yes/no)	0/9	4/202	1.000	0.957 (0.930–0.985)
PT-INR >1.5 (yes/no)	7/2	11/195	<0.001	62.045 (11.509–334.498)
Platelet count <100000/μl (yes/no)	4/5	28/178	0.030	5.086 (1.287–20.091)
WBC count >12000 or <4000/μl (yes/no)	4/5	58/148	0.284	2.041 (0.530–7.870)
CRP ≥5 mg/dl (yes/no)	6/3	75/131	0.084	3.494 (0.849–14.375)
Serum albumin level ≤2.8 g/dl (yes/no)	8/1	32/174	<0.001	43.500 (5.259–359.751)
T-Bil ≥5 mg/dl (yes/no)	6/3	93/113	0.307	0.412 (0.100–1.690)
Body temperature >38 °C or <36 °C (yes/no)	3/6	87/119	0.737	0.684 (0.166–2.810)
Etiology (malignant/benign)	4/5	105/101	0.746	1.300 (0.399–4.977)
Age ≥75 years (yes/no)	2/7	55/151	1.000	0.784 (0.158–3.891)
Inpatient/outpatient	5/4	99/107	0.742	1.351 (0.353–5.175)
Stent dysfunction (yes/no)	4/5	74/132	0.726	1.427 (0.372–5.497)

mortality. Therefore, severe acute cholangitis, i.e., cholangitis accompanied by organ dysfunction, should be treated immediately using EBD, as recommended by the TG07.

Before the TG07 were published, Charcot's triad (criterion 1) was recognized as the definitive criterion for diagnosing acute cholangitis. The accuracy rate of Charcot's triad as a diagnostic criterion was reported to be up to 72 % [5]. In the present study, the overall incidence of Charcot's triad was relatively low (33.4 %, 72/215). Moreover, the incidence of Charcot's triad increased according to disease severity (mild, moderate, severe; 7.7 vs. 39.8 vs. 50 %, respectively; $p < 0.001$). Therefore, the incidence of Charcot's triad may depend on the severity of acute cholangitis. Similarly, CRP value may be a useful factor in severity assessment of cholangitis as shown in that of acute pancreatitis [9], however, cut-off value (CRP ≥5.0 mg/dl) based on the ROC analysis did not show ideal sensitivity or specificity. Theoretically, mild cholangitis should account for the largest proportion of cases; however, in this study, more cases of moderate cholangitis were observed. In some cases, mild cholangitis may have resolved on its own before detection, leading to underdiagnosis. In addition, information on physical findings, laboratory results, or imaging may have been lost or not examined when acute cholangitis was not considered as part of the differential diagnosis.

Assessments of disease severity according to the TG07 have an important limitation: the definition of moderate cholangitis is vague. Moderate cholangitis is defined as disease unresponsive to initial conservative medical treatment, meaning that a conclusive severity assessment must be deferred until conservative treatment fails. From the clinical point of view, more reliable markers are required for predicting the deterioration of cholangitis. The results of this study showed that hypoalbuminemia (≤2.8 g/dl) and increased PT-INR (>1.5) were statistically significant predictors of mortality. According to the TG07, increased PT-INR occurs because of organ dysfunction. In such cases, urgent biliary drainage is recommended. However, hypoalbuminemia is listed as only one of many prognostic factors [3–5]. Hypoalbuminemia, which is a host-related risk factor, has been shown to have an adverse effect on outcome in patients with or without acute cholangitis requiring emergency surgery for intra-abdominal infection [10, 11]. In cases of acute cholangitis with hypoalbuminemia but without organ dysfunction, early endoscopic drainage should be performed without waiting for the outcome of conservative medical treatment. In the current study, host-related factors associated with hypoalbuminemia were not clarified. Future research should explore this issue.

Previous reports that analyzed cases of severe acute cholangitis documented various risk factors and advocated their own scoring systems [12–15]. The most common

Table 8 Multivariate analysis with regard to mortality

Variables	Odds ratio	(95 % CI)	*p* value
Serum albumin level ≤2.8 g/dl	15.9	(1.7–142.9)	0.017
PT-INR >1.5	22.7	(3.7–142.9)	0.001

Table 9 Results of univariate analysis with regard to refractory cholangitis

Factor	Refractory ($n = 57$)	Not refractory ($n = 158$)	*p* value	OR (95 % CI)
Hypotension requiring dopamine ≥5 μl/kg per min or any dose of dobutamine (yes/no)	11/46	8/150	0.002	4.484 (1.702–11.813)
Disturbance of consciousness (yes/no)	9/48	8/150	0.019	3.516 (1.285–9.617)
PaO_2/FiO_2 ratio <300 (yes/no)	6/51	3/155	0.012	6.078 (1.467–25.186)
Serum creatinine >2.0 mg/dl (yes/no)	1/56	3/155	1.000	0.923 (0.094–9.054)
PT-INR >1.5 (yes/no)	10/47	8/150	0.009	3.989 (1.489–10.691)
Platelet count <100000/μl (yes/no)	12/45	20/138	0.134	1.840 (0.834–4.058)
WBC count >12000 or <4000/μl (yes/no)	14/43	48/110	0.496	0.746 (0.374–1.490)
CRP ≥5 mg/dl (yes/no)	21/36	60/98	1.000	0.953 (0.509–1.783)
Serum albumin level ≤2.8 g/dl (yes/no)	20/37	20/138	0.001	3.730 (1.819–7.649)
T-Bil ≥5 mg/dl (yes/no)	38/19	78/80	0.030	2.051 (1.089–3.863)
Body temperature >38 or <36 °C (yes/no)	23/34	67/91	0.876	0.919 (0.496–1.701)
Etiology (malignant/benign)	44/13	62/96	<0.001	5.241 (2.612–10.514)
Age ≥75 years (yes/no)	14/43	43/115	0.730	0.871 (0.433–1.749)
Inpatient/outpatient	44/13	60/98	<0.001	5.528 (2.753–11.101)
Stent dysfunction (yes/no)	30/27	48/110	0.004	2.546 (1.369–4.737)

Table 10 Multivariate analysis with regard to refractory cholangitis

Variables	Odds ratio	(95 % CI)	*p* value
Serum albumin level ≤2.8 g/dl	2.4	(1.02–5.56)	0.045
PT-INR >1.5	4.8	(1.39–16.39)	0.013
Etiology (malignant)	4.3	(1.94–9.43)	<0.001
Inpatient	4.3	(1.96–9.35)	<0.001

etiology of severe acute cholangitis in those studies was choledocholithiasis. In contrast, malignant disease was the most common etiology of moderate and severe cholangitis in the present study (63.8 %, 104/163). In total, 67 % cases (71/106) with malignant biliary strictures in the present study had previously received in situ plastic or metal stent implantation. Recent developments in chemotherapy for advanced pancreatic or biliary cancer have improved survival with the help of endoscopic stent placement. Although studies have compared the patencies of various stents [16, 17], few make mention of the frequency of stent-associated acute cholangitis and its management [18]. Patients with biliary stents placed in situ are at a higher risk of septic acute cholangitis compared with those without stents [19]. Our results showed that both stent dysfunction and etiology (malignant) were not significant predictors of mortality. In the present study, all cases with stent dysfunction were included under the category of moderate or severe cholangitis following immediate biliary drainage. Early EBD may prevent further deterioration of cholangitis, even in such high-risk patients.

In this study, 48 cases required >28-day hospitalization after having received EBD. Survival in these cases may be attributed to immediate biliary drainage following intensive conservative medical treatment. Multivariate analysis in our study showed that increased PT-INR, hypoalbuminemia, etiology (malignancy), and inpatient status were significant risk factors for refractory cholangitis. All predictors except increased PT-INR were host-related factors. Therefore, when acute cholangitis develops in a hospital inpatient with hypoalbuminemia or malignancy, EBD should be performed.

The limitations of this study were that it was retrospective and conducted on a small number of cases at a single institution.

In conclusion, severe acute cholangitis, defined as cholangitis complicated with organ dysfunction, should be treated immediately using EBD, as recommended by the TG07. For cases of acute cholangitis with hypoalbuminemia but without accompanying organ dysfunction, early EBD should be performed without waiting for a response to conservative medical treatment. A multicenter prospective study should be undertaken to confirm the usefulness of hypoalbuminemia as a predictor of poor outcome.

References

1. Kimura Y, Takada T, Kawarada Y, Nimura Y, Hirata K, Sekimoto M, et al. Definitions, pathophysiology, and epidemiology of acute cholangitis and cholecystitis: Tokyo Guidelines. J Hepatobiliary Pancreat Surg. 2007;14:15–26.
2. Thompson J, Bennion RS, Pitt HA. An analysis of infectious failures in acute cholangitis. HPB Surg. 1994;8:139–44 (discussion 145).
3. Csendes A, Diaz JC, Burdiles P, Maluenda F, Morales E. Risk factors and classification of acute suppurative cholangitis. Br J Surg. 1992;79:655–8.
4. Nishino T, Onizawa S, Hamano M, Shirato I, Shirato M, Hamano T, et al. Proposed new simple scoring system to identify indications for urgent ERCP in acute cholangitis based on the Tokyo Guidelines. J Hepatobiliary Pancreat Sci. 2011 (Epub ahead of print).
5. Wada K, Takada T, Kawarada Y, Nimura Y, Miura F, Yoshida M, et al. Diagnostic criteria and severity assessment of acute cholangitis: Tokyo Guidelines. J Hepatobiliary Pancreat Surg. 2007;14:52–8.
6. Miura F, Takada T, Kawarada Y, Nimura Y, Wada K, Hirota M, et al. Flowcharts for the diagnosis and treatment of acute cholangitis and cholecystitis: Tokyo Guidelines. J Hepatobiliary Pancreat Surg. 2007;14:27–34.
7. Tsuyuguchi T, Takada T, Kawarada Y, Nimura Y, Wada K, Nagino M, et al. Techniques of biliary drainage for acute cholangitis: Tokyo Guidelines. J Hepatobiliary Pancreat Surg. 2007;14:35–45.
8. Lai EC, Mok FP, Tan ES, Lo CM, Fan ST, You KT, et al. Endoscopic biliary drainage for severe acute cholangitis. N Engl J Med. 1992;326:1582–6.
9. Hirota M, Takada T, Kawarada Y, Hirata K, Mayumi T, Yoshida M, et al. JPN Guidelines for the management of acute pancreatitis: severity assessment of acute pancreatitis. J Hepatobiliary Pancreat Surg. 2006;13:33–41.
10. Lai EC, Tam PC, Paterson IA, Ng MM, Fan ST, Choi TK, et al. Emergency surgery for severe acute cholangitis. The high-risk patients. Ann Surg. 1990;211:55–9.
11. Pacelli F, Doglietto GB, Alfieri S, Piccioni E, Sgadari A, Gui D, et al. Prognosis in intra-abdominal infections. Multivariate analysis on 604 patients. Arch Surg. 1996;131:641–5.
12. Gigot JF, Leese T, Dereme T, Coutinho J, Castaing D, Bismuth H. Acute cholangitis. Multivariate analysis of risk factors. Ann Surg. 1989;209:435–8.
13. Hui CK, Lai KC, Yuen MF, Ng M, Lai CL, Lam SK. Acute cholangitis-predictive factors for emergency ERCP. Aliment Pharmacol Ther. 2001;15:1633–7.
14. Rosing DK, De Virgilio C, Nguyen AT, El Masry M, Kaji AH, Stabile BE. Cholangitis: analysis of admission prognostic indicators and outcomes. Am Surg. 2007;73:949–54.
15. Salek J, Livote E, Sideridis K, Bank S. Analysis of risk factors predictive of early mortality and urgent ERCP in acute cholangitis. J Clin Gastroenterol. 2009;43:171–5.
16. Katsinelos P, Kountouras J, Chatzimavroudis G, Zavos C, Paroutoglou G, Pilpilidis I, et al. A novel technique of injection treatment for endoscopic sphincterotomy-induced hemorrhage. Endoscopy. 2007;39:631–6.

17. Kullman E, Frozanpor F, Soderlund C, Linder S, Sandstrom P, Lindhoff Larsson A, et al. Covered versus uncovered self-expandable nitinol stents in the palliative treatment of malignant distal biliary obstruction: results from a randomized, multicenter study. Gastrointest Endosc. 2010;72:915–23.
18. Buxbaum JL, Biggins SW, Bagatelos KC, Inadomi JM, Ostroff JW. Inoperable pancreatic cancer patients who have prolonged survival exhibit an increased risk of cholangitis. JOP. 2011;12:377–83.
19. Rerknimitr R, Fogel EL, Kalayci C, Esber E, Lehman GA, Sherman S. Microbiology of bile in patients with cholangitis or cholestasis with and without plastic biliary endoprosthesis. Gastrointest Endosc. 2002;56:885–9.

Intrahepatic Cholangiocarcinoma With Predominant "Ductal Plate Malformation" Pattern

A New Subtype

Yasuni Nakanuma, MD, PhD, Yasunori Sato, MD, PhD,* Hiroko Ikeda, MD, PhD,† Kenichi Harada, MD, PhD,* Mikiko Kobayashi, MD,‡ Kenji Sano, MD, PhD,‡ Takeshi Uehara, MD, PhD,‡ Masakazu Yamamoto, MD, PhD,§ Shunichi Ariizumi, MD,§ Young Nyun Park, MD, PhD,‖ Joon Hyuk Choi, MD, PhD,¶ and Ensil Yu, MD, PhD#*

Abstract: Ten cases of intrahepatic cholangiocarcinoma showing a highly differentiated adenocarcinoma mimicking ductal plate malformation (DPM) are reported. The patients included 7 males and 3 females with an average age of 69.5 years. Six cases were associated with chronic liver disease and the remaining 4 cases showed mild fatty change in the parenchyma and/or minimal to mild portal inflammation. Grossly, the tumor was a single nodule 1.5 to 6.6 cm in diameter, and was whitish and solid without a fibrous capsule. Microscopically, the tumor was composed of many vague, small nodular carcinomatous areas with desmoplastic reactions, and neoplastic glands had an irregularly dilated lumen lined with a single layer of cuboidal or low columnar carcinoma cells and irregular protrusions and bulges, resembling DPM. At its border, the carcinoma seemed to replace the non-neoplastic hepatic lobules or regenerative nodules. The central parts of the tumor were variably hypocellular and fibrotic. Although these carcinomas were negative for mucin and HepParI, they were frequently positive for CK19, epithelial cell adhesion molecule, and epithelial membrane antigen. Neural cell adhesion molecule was also expressed variably. The Ki-67 labeling index was < 10% and p53 was scarcely expressed. In conclusion, a new subtype of intrahepatic cholangiocarcinoma with predominant DPM pattern was identified.

Key Words: cholangiocarcinoma, ductal plate malformation, cholangiocytes, bile ductular carcinoma

(*Am J Surg Pathol* 2012;36:1629–1635)

From the *Department of Human Pathology, Kanazawa University Graudate School of Medicine; †Diagnostic Pathology Section, Kanazawa University Hospital, Kanazawa; ‡Department of Pathology, Shinshu University School of Medicine, Matsumoto, Nagano; §Department of Surgery, Tokyo Women's Hospital, Tokyo, Japan; ‖Department of Pathology, Yonsei University School of Medicine, Seoul; #Department of Pathology, Asan Medical Center, Medical College of Ulsan, Seoul; and ¶Department of Pathology, Yeungnam University College of Medicine, Daegu, Korea.

Conflicts of Interest and Source of Funding: The authors have disclosed that they have no significant relationships with, or financial interest in, any commercial companies pertaining to this article.

Correspondence: Yasuni Nakanuma, MD, PhD, Department of Human Pathology, Kanazawa University Graduate School of Medicine, Kanazawa 920-8640, Japan (e-mail: pbcpsc@kenroku.kanazawa-u.ac.jp).

Intrahepatic cholangiocarcinomas (ICCs) are usually well to moderately differentiated adenocarcinomas, and show a tubular or micropapillary structure with a desmoplastic stroma.[1,2] They are usually positive for mucin. The histogenesis of peripheral ICC remains controversial.[3,4] However, a subgroup of peripheral ICCs comprises a highly differentiated adenocarcinoma composed of malignant neoplastic glands having a lumen that is usually indistinct and showing an infiltrating replacement growth pattern against the surrounding liver. Their features resemble those of reactive bile ductules.[1,3–9] They usually express neural cell adhesion molecule (NCAM) and epithelial cell adhesion molecule (EpCAM) at the basolateral surface and their luminal surface is positive for epithelial membrane antigen (EMA). "Bile ductular carcinoma" or cholangiolocellular carcinoma has been proposed as a better term for this subgroup,[4–7] and their histogenesis could be related to hepatic progenitor cells or stem cells located at bile ductules or canals of Hering in the liver.[10]

We recently noticed that some peripheral ICCs exhibit peculiar histologic features, resembling ductal plate malformation (DPM), an abnormal biliary and stromal malformation characteristically found in patients with Caroli disease and congenital hepatic fibrosis (CHF) or in PCK rats.[8,11–14] This DPM is characterized by an irregularly shaped and variably dilated glands covered by a low columnar or cuboidal biliary epithelium, bulging or irregular protrusions covered by biliary epithelium into the dilated lumen, and bridge-like structures covered by biliary epithelium in the dilated lumen (Fig. 1). Dilated and continuous DPM occasionally surrounds part or all of the portal tract.

Herein, we describe in detail the pathologic features of these 10 cases with the help of immunohistochemistry and characterize ICC with predominant DPM pattern as a new subtype.

MATERIALS AND METHODS

Case Selection

A total of 10 ICCs with predominant DPM pattern were obtained in our Medical Centers, and the gross and histologic changes of the tumor and non-neoplastic livers

FIGURE 1. Ductal plate malformation in congenital hepatic fibrosis. Duct structures in the periportal area are irregularly dilated, with some showing bridging, and some part of portal tract (*) is surrounded by dilated ducts (HE).

were examined in tumor specimens with surrounding non-neoplastic liver. All were surgically resected specimens. The staging of nonalcoholic steatohepatitis (NASH) and chronic viral hepatitis were done according to the NASH Clinical Research Network Scoring System[15] and METAVIR system.[16]

In this study, the ICC cases showing DPM pattern in more than half of the tumor area were included, and this DPM pattern was similar to the benign DPM described above and differed from the micropapillary structures found in adenocarcinomas.

Histologic Observation and Immunohistochemistry

All of the liver specimens including the tumor were fixed in 10% formalin and embedded in paraffin. In 4 cases, only hematoxylin and eosin sections were available, and in the remaining 6 cases, more than 10 serial thin sections, 4 μm in thickness, were prepared. After deparaffinization, thin sections were stained with hematoxylin and eosin, Azan-Mallory, and periodic acid Schiff after diastase digestion (di-PAS) for histologic observation. The remaining sections were used for immunohistochemistry.

Immunohistochemistry

Immunohistochemistry was performed with an EnVision+ system (Dako, Glostrup, Denmark) and primary antibodies such as HepParI as a marker of human hepatocyte or hepatocellular carcinoma (HCC) (clone OCH1E5, mouse monoclonal, optimal dilution 1:100; Dako), CD56 as a marker of NCAM (clone QBEND10, mouse monoclonal, 1:200; Immunotech, Marseille, France), EpCAM (clone HEA 125, mouse monoclonal antibody, 1:5; Ab cam, Tokyo, Japan), EMA (clone M613, mouse monoclonal, 1:200; Dako), cytokeratin (CK) 19 (1:100; Dako), p53 (clone DO-7, mouse monoclonal, 1:100; Dako) and Ki67 (clone MIB1, mouse monoclonal, 1:200; Dako). After deparaffinization, antigen retrieval was performed for CK19 and HepParI by microwaving in 10 mM citrate buffer, pH 6.0 for 20 minutes. CK19 was incubated in the 0.1% trypsin retrieval solution at 37°C for 15 minutes. After the blocking of endogenous peroxidase, deparaffinized sections were incubated overnight at 4°C with the primary antibodies. Then, the sections were incubated with secondary antibodies conjugated to a peroxidase-labeled polymer (EnVision+ system; Dako). After a reaction with benzidine, the sections were counterstained lightly with hematoxylin. Negative controls were made by substituting the primary antibody with nonimmunized mouse IgG. In non-neoplastic liver, hepatocytes were positive for HepParI, nerve fibers for NCAM, bile ductules for EMA, and interlobular bile ducts for CK19 and EpCAM, so these tissue elements were used as internal positive controls. As a positive control for p53 and Ki-67, 2 cases of moderately differentiated adenocarcinoma of the colon were used.

Labeling Index for Ki-67

Ki-67 expression was evaluated in more than 500 carcinoma cells in several areas of carcinoma with the DPM pattern, and the percentage of positive cells was expressed as the Ki-67 LI.

RESULTS

Gross Features

A total of 10 patients were examined (7 males and 3 females) with an average age of 69.5 years (53 to 81 y) (Table 1). Six cases were associated with chronic liver disease [1 case of NASH with stage 2 and NAS (nonalcoholic fatty liver disease activity) score 4; 2 cases of alcoholic steatohepatitis with severe hepatic fibrosis; 2 cases of chronic viral hepatitis B (F3/A1 and F4/A1, respectively); and 1 case of chronic viral hepatitis C (F4/A1)], whereas the background liver in the remaining 4 cases was almost normal except for mild fatty deposition in the parenchyma and/or a few inflammatory cells in the portal tracts. Tumors with predominant DPM pattern were singular, and found in the left lobe in 3 cases and in the right lobe in 7 cases (Table 1). They ranged from 1.5 to 6.6 cm in greatest diameter. These tumors were a whitish or gray solid nodule with a relatively clear but slightly vague border, but had no capsule, and were round or elliptical with or without several small bulges against the surrounding liver (Fig. 2). They were elastic hard and showed no grossly visible cystic changes within. The tumors were homogenous, although the central parts were rather hyalinous in 6 cases. After formalin fixation, a few focal and small green tint or vague spots were found at the periphery of the tumor in 2 cases.

Histologic Features

These tumor nodules had no capsule. Under lower magnification, the carcinomas were composed of many vague, small nodular areas, particularly in the peripheral

TABLE 1. Major Findings of 10 Cases of ICC With Predominant DPM Pattern

Cases	Age/ Sex	Background Liver	Location of the Tumor in Liver	Size of the Tumor	Proportion of DPM Pattern (%)*	Ki-67 LI	Other Neoplastic Lesions in Liver
Case 1	60s/M	HBV-related chronic hepatitis (F3/A1)	Right lobe	1.7 × 1 cm	70	ND	ICC
Case 2	70s/F	Mild fatty deposition	Left lobe	3.6 × 3.4 cm	70	ND	None
Case 3	80s/M	NASH stage 2	Right lobe	2.5 × 2.5 cm	90	4.9%	None
Case 4	60s/M	Alcoholic steatohepatitis severe fibrosis	Right lobe	1.0 × 0.9 cm	80	1.3%	None
Case 5	70s/M	HBV-related chronic hepatitis (F4/A1)	Left lobe	3.5 × 3.5 cm	60	2.4%	None
Case 6	70s/F	Mild portal inflammation	Right lobe	1.5 × 1.0 cm	70	ND	None
Case 7	70s/M	Alcoholic steatohepatitis severe fibrosis	Left lobe	1.7 × 1.3 cm	60	9.6%	HCC, bile duct adenoma
Case 8	50s/F	Mild portal inflammation	Right lobe	6.6 × 6.6 cm	80	2.7%	HCC
Case 9	60s/M	HCV-related chronic hepatitis (F4/A1)	Right lobe	1.5 × 1.5 cm	70	6.0%	None
Case 10	60s/M	Mild steatosis and mild portal inflammation	Right lobe	4.5 × 3.5 cm	90	ND	None

*Part(s) of the tumor other than those showing a DPM pattern are compared with bile ductular carcinoma and occasional foci of ordinary ICC.
F indicates female; HBV, hepatitis B virus; HCV, hepatitis C virus; M, male; ND, not done.

parts (Fig. 3A). These nodular areas, which were surrounded or divided by fibrous bands, were composed of neoplastic glands with an irregularly dilated lumen with desmoplastic reactions (Figs. 3B, C), whereas the central areas were hypocellular and more fibrotic and even hyalinous. At the borders, the carcinoma replaced the adjacent hepatic parenchyma, and some hepatic lobules or regenerative nodules were replaced by carcinoma cells (Fig. 3D) and small remnants of hepatic parenchyma were occasionally entrapped within nodular carcinomatous areas. Interestingly, portal tracts and hepatic vein tributaries were distributed rather regularly, and portal tracts with a patent vascular lumen were found within the tumor (Figs. 3A, E). The combination of multiple small nodular growth patterns of carcinoma and rather regular distribution of portal tracts and hepatic vein tributaries in the tumor suggests that the preexisting framework of hepatic lobules or regenerative nodules was replaced by carcinoma cells (Figs. 3A, D, E), and the portal tracts and hepatic vein tributaries might remain incorporated secondarily within the tumor.

More than half of these carcinomatous areas were composed of carcinoma showing a DPM pattern (Figs. 3B–F). This pattern was characterized by neoplastic glands of carcinoma showing an irregularly shaped and dilated lumen, and some of these glands showed microcystic dilatation (Fig. 3C). Neoplastic glands with the DPM pattern were lined by a single layer of cuboidal or low columnar carcinoma cells with clear and scanty cytoplasm (Fig. 3F), and the nuclei were small and mildly hyperchromatic. There was no anisonucleosis or anisocytosis, and mitoses were rare or absent. Irregular protrusions and bridging structures of carcinoma with fibrous stroma in the dilated lumen were also scattered as seen in benign DPM. Their features are different from the micropapillary structures found in conventional adenocarcinomas. Occasionally, condensed bile plugs were found in the dilated lumen of neoplastic glands with the DPM pattern adjacent to the adjoining or entrapped hepatic parenchyma (Figs. 3D, G). These bile plugs were considered entrapped bile.

In addition, several bile ductular carcinomatous areas resembling reactive bile ductules without a distinct lumen and with cuboidal or low columnar cells[3,5,7] were admixed focally within these carcinomas with DPM pattern in all cases (Fig. 3G). Small foci of ordinary ICC were also found within these carcinomas in 3 cases (cases 5, 8, and 10 in Table 1; Figs. 3H, I). The proportion of carcinoma with the DPM pattern within the tumor nodule is shown in Table 1; parts other than this DPM

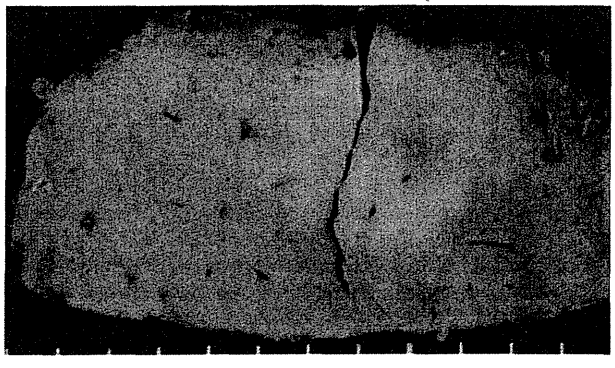

FIGURE 2. A whitish nodular tumor with an irregular and slightly vague border is found in an apparently normal liver. A green tint is evident at the peripheral parts of the tumor.

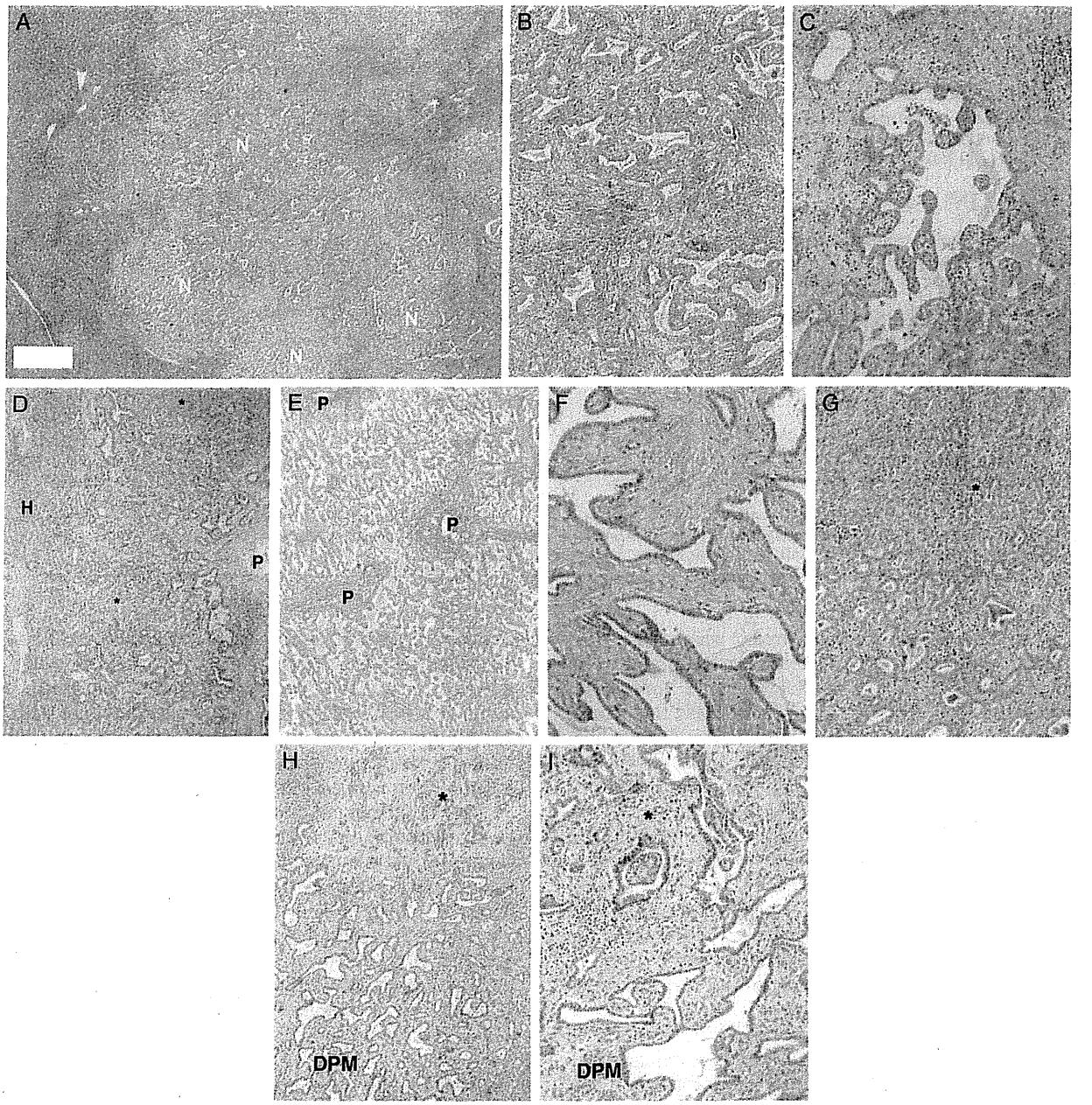

FIGURE 3. A, The tumor is composed of many vague, smaller nodular areas (N) that are subdivided or surrounded by fibrous tissue in the peripheral area, whereas the central parts are more hypocellular and more fibrotic (*) (Azan-Mallory stain). B, The nodular areas of carcinoma are composed of neoplastic glands with an irregularly dilated lumen, resembling DPM (DPM pattern), and are surrounded or divided by fibrous bands (Azan-Mallory stain). C, Some carcinomas with a DPM pattern have a microcystic appearance (HE). D, In the peripheral part of carcinoma, carcinoma cells with DPM pattern replace hepatic parenchyma and small foci of hepatic parenchyma is entrapped within carcinoma (*). Bile is entrapped in the dilated lumen of the adenocarcinoma composed by the malignant neoplastic glands (HE). E, Portal tracts (P) are identifiable regularly within carcinoma (Gomori's reticulin stain). F, Carcinoma with DPM pattern and desmoplastic reaction is recognizable and the malignant neoplastic glands that compose the adenocarcinoma are lined by a single layer of cuboidal or low columnar epithelial cell (HE). G, Some parts of carcinoma with DPM pattern (lower half) are in continuity with bile ductular carcinoma without a distinct lumen (*). In the former, bile is in the dilated lumen of the adenocarcinoma composed by the malignant neoplastic glands with DPM pattern (HE). H, Carcinoma with the DPM pattern is continuous with ordinary cholangiocarcinoma (*) (HE). I, Carcinoma with the DPM pattern in continuous with ordinary cholangiocarcinoma (*) (HE).

pattern were bile ductular carcinoma and/or ICC showing well to moderately differentiated adenocarcinoma.

Background Liver

Cirrhosis or advanced liver disease was found in 6 of 10 cases examined, whereas the remaining 4 livers were almost normal except for mild fatty deposition in the parenchyma and/or minimal or mild portal inflammation (Table 1). A solitary HCC nodule (1.6 cm in diameter) with moderate differentiation and bile duct adenoma (0.6 cm) were found in other parts of the liver in case 7, a solitary HCC nodule (3 cm) with moderate differentiation in case 8, and a solitary ICC nodule of moderately differentiated adenocarcinoma (2.8 cm) in case 1. These tumors were not in continuity with ICC with the DPM pattern in the liver.

Histochemistry and Immunohistochemistry

In the carcinoma areas showing the DPM pattern, the carcinomas were negative for di-PAS, however some macrophages, which were located in the lumen in neoplastic glands, were positive (Fig. 4A). EMA was clearly expressed on the luminal side of the neoplastic glands in carcinomas with the DPM pattern. EpCAM was expressed on the basolateral surface of the neoplastic glands in all cases of carcinomas with the DPM pattern. CK19 was also diffusely expressed in the cytoplasm in the neoplastic glands. NCAM was positive on the basolateral surface of these neoplastic cells in all cases (Fig. 4B). HepParI was absent in these carcinomatous areas, although entrapped hepatocytes within the tumor were clearly positive for HepParI. As for proliferative activities, Ki-67 LI ranged from 1.3% to 9.8% (4.5% ± 2.8%) (Table 1). p53 expression in nuclei was scarce in carcinoma with the DPM pattern in all cases.

Some areas of ordinary ICCs were focally positive for di-PAS, whereas bile ductular carcinoma foci were negative. As for the expression of EMA, EpCAM, CK19, NCAM, and HepParI, bile ductular carcinoma foci showed similar results as seen in ICC with the DPM pattern.

The results can be summarized as follows: (i) 10 cases of peripheral ICC showed solid growth and were composed of many small, vague nodular areas mainly in the peripheral regions, and these nodular carcinomatous areas showed predominantly a DPM pattern with an irregularly shaped and dilated lumen. Central areas were mainly hypocellular and more fibrotic. (ii) These patients were all adults and predominantly male, and 6 cases arose on a background of chronic liver disease. (iii) Carcinomas with the DPM pattern were diffusely positive for EMA, CK19, and EpCAM, and variably positive for NCAM, but negative for di-PAS and HepParI. The Ki-67 labeling index (LI) was low, and p53 was scarcely positive in nuclei.

DISCUSSION

The pathologic features of ICC are generally heterogenous, and this heterogeneity may reflect the histology and phenotypes of the anatomic location of the biliary tree from which the ICC might have developed.[1–3,9] Perihilar ICCs arising from the intrahepatic large bile duct including peribiliary glands may secrete mucin and show a large lumen or papillary patterns.[1,2,17] Other ICCs arising from the bile ductules/canals of Hering, where hepatic progenitor cells are located,[5–7,10] present as a mass-forming type and show features and phenotypes of reactive bile ductules. Some of the latter ICCs are composed of neoplastic glands having an indistinct lumen and abundant fibrous stroma and could be called bile ductular carcinoma or cholangiolocellular carcinoma.[5–7] Although the cases presented here may belong to the latter ICC, a majority of the tumor areas were uniquely composed of carcinoma with DPM pattern.

The ductal plate, a unique structure found in the fetal liver, disappears with the remodeling of the intrahepatic bile ducts and is not found in postnatal liver.[18] Desmet and colleagues reported that some postnatal diseases present with several features of this ductal plate.[2,19,20] They referred to such pathologic features as DPM (Fig. 1). DPM is found in cases of CHF, Caroli disease, and other fibropolycystic diseases.[2,19,20] As for the genetic and molecular mechanisms of DPM occurring in patients with Caroli disease and CHF, disordered cell kinetics of biliary epithelial cells such as the activation of the MEK5-ERK5 cascade were reportedly involved.[13,21] In addition, basal laminar components and stromal fibrogenesis may play important roles. Biliary overexpression of plasminogen and tissue-type plasminogen activator leads to the generation of excessive amounts of plasmin, and subsequent plasmin-dependent lysis of the extracellular matrix molecules may contribute to the formation of DPM in CHF and Caroli disease.[22,23] In addition, several genetic changes involving hepatocyte nuclear factor (HNF)-6, HNF1β, and cystin were reported to be involved in the DPM process in animal models.[24]

More than half of the tumor area in our ICC cases exhibited the DPM pattern. Interestingly, such a pattern has been also reported in some hamartomatous or neoplastic diseases such as the Von Meyenburg complex and mesenchymal hamartoma.[1,6,7] Although the mechanisms for the development of the DPM pattern in ICC and other neoplastic diseases remain speculative, the genetic and molecular alterations reported in CHF and Caroli diseases[13,21–24] may also operate in ICC with the DPM pattern. Further study of the genetic alterations speculated in benign DPM is warranted to clarify this unique morphogenesis of ICC with the DPM pattern.

Interestingly, the ICCs with the DPM pattern in this series expressed hepatic progenitor cell markers such as EpCAM, EMA, NCAM, and CK19 that were also present in the reactive bile ductules in non-neoplastic liver diseases and also bile ductular carcinoma.[6,11,13,19,20] However, they were negative for mucin staining or HepParI. Furthermore, foci of bile ductular carcinomas without a distinct lumen were also present in all ICC cases with the DPM pattern. For the development of bile ductular carcinoma, hepatic progenitor cells or neoplastic

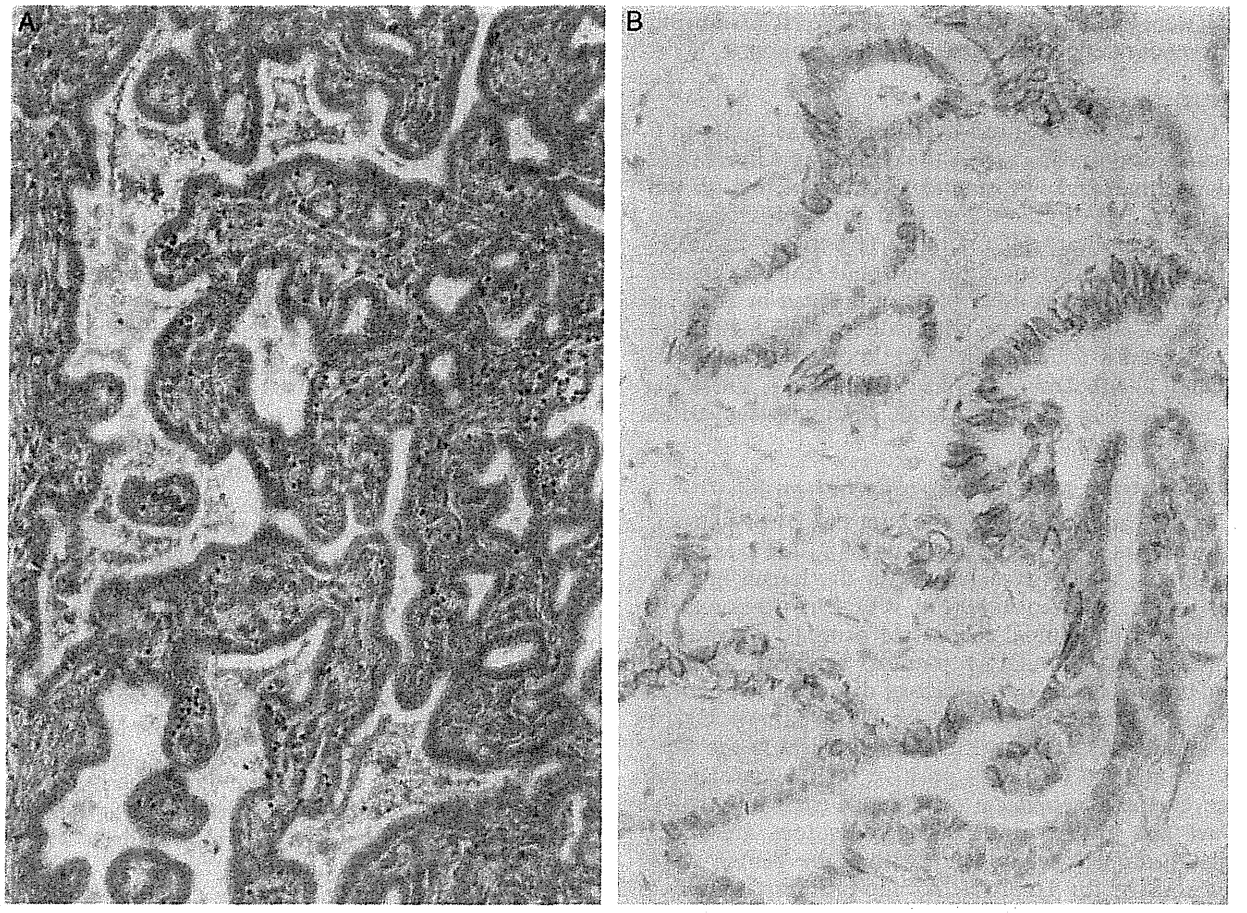

FIGURE 4. A, Carcinomas showing a DPM pattern are negative for di-PAS except for some positive macrophages that are located in the lumen of the neoplastic glands. B, NCAM is expressed on the basolateral surface of carcinoma, with the DPM pattern. Immunostaining for NCAM with hematoxylin counterstain.

cells with characteristics of hepatic progenitor cells are presumed to be involved.[5,6,7] Taken together, the carcinomas with the DPM pattern presented here may retain progenitor cell features.[5,6,7] The ICC with predominant DPM pattern described in this study has not been reported so far, and in this context, this type with progenitor cell phenotypes could be regarded as a subtype of ICC.

Clinical studies showed that bile ductular carcinoma has a slightly better prognosis after surgical resection than ordinary ICC.[25] Interestingly, in 3 of our 10 cases, small foci of ordinary ICC were found within the tumor and were in continuity with carcinoma showing the DPM pattern. The Ki-67 LI was 4.5% ± 2.8% and p53 expression was scarce in ICC with the DPM pattern, and these data were lower in comparison with ordinary ICC in which the Ki-67 LI was >25% and p53 LI was >20%.[26] The occurrence of ordinary ICC was also reported in bile ductular carcinoma.[6,7] Therefore, it seems possible that ordinary ICC may arise in ICC with the DPM pattern, although such tumors may simply demonstrate multiple morphologic patterns. More studies are needed to verify this speculation.

Finally, it is necessary to differentiate the DPM pattern in ICC from benign DPM such as Von Meyenburg complex and CHF. At present, cellular and nuclear features may help such differentiation in needle core specimens. In our experience, the neoplastic cells lining the DPM in the former are larger and monotonous in comparison with the biliary cells lining the DPM in the latter. Further immunohistochemical study may be necessary to settle this issue.

In conclusion, peripheral ICCs showing predominantly DPM pattern were reported. Such tumors have not been reported previously, and may be a new subtype of ICC. Some of the genetic factors involved in the formation of benign DPM may be also responsible for the formation of the DPM pattern in ICC. More clinicopathologic and genetic studies using more cases are needed to characterize this peculiar subtype of ICC.

REFERENCES

1. Nakamura Y, Curabo MP, Franceschi S, et al. *Intrahepatic Cholangiocarcinoma.* 4th ed. Lyon: World Health Organization of Tumours; 2010.

2. Nakanuma Y, Sato Y, Harada K, et al. Pathological classification of intrahepatic cholangiocarcinoma based on a new concept. *World J Hepatol.* 2010;2:419–427.
3. Komuta M, Govaere O, Vandecaveye V, et al. Histological diversity in cholangiocellular carcinoma reflects the different cholangiocyte phenotypes. *Hepatology.* 2012;55:1876–1888.
4. Sempoux C, Fan C, Singh P, et al. Cholangiolocellular carcinoma: an innocent-looking liver tumor mimicking ductular reaction. *Semin Liver Dis.* 2011;31:104–110.
5. Komuta M, Spee B, Vander Borght S, et al. Clinicopathological study on cholangiolocellular carcinoma suggesting hepatic progenitor cell origin. *Hepatology.* 2008;47:1544–1556.
6. Kozaka K, Sasaki M, Fujii T, et al. A subgroup of intrahepatic cholangiocarcinoma with an infiltrating replacement growth pattern and a resemblance to reactive proliferating bile ductules: 'bile ductular carcinoma'. *Histopathology.* 2007;51:390–400.
7. Nakanuma Y, Sasaki M, Ikeda H, et al. Pathology of peripheral intrahepatic cholangiocarcinoma with reference to tumorigenesis. *Hepatol Res.* 2008;38:325–334.
8. Nakanuma Y, Terada T, Ohta G, et al. Caroli's disease in congenital hepatic fibrosis and infantile polycystic disease. *Liver.* 1982;2:346–354.
9. Sempoux C, Jibara G, Ward SC, et al. Intrahepatic cholangiocarcinoma: new insights in pathology. *Semin Liver Dis.* 2011;31:49–60.
10. Roskams T. Liver stem cells and their implication in hepatocellular and cholangiocarcinoma. *Oncogene.* 2006;25:3818–3822.
11. Jain D, Sarode VR, Abdul-Karim FW, et al. Evidence for the neoplastic transformation of Von-Meyenburg complexes. *Am J Surg Pathol.* 2000;24:1131–1139.
12. Nakamura Y, Zen Y, Portman B. *Diseases of the Bile Ducts.* 6th ed. Edinburg: Churchill Livingstone; 2011.
13. Sanzen T, Harada K, Yasoshima M, et al. Polycystic kidney rat is a novel animal model of Caroli's disease associated with congenital hepatic fibrosis. *Am J Pathol.* 2001;158:1605–1612.
14. Desmet VJ. Congenital diseases of intrahepatic bile ducts: variations on the theme "ductal plate malformation". *Hepatology.* 1992;16:1069–1083.
15. Kleiner DE, Brunt EM, Van Natta M, et al. Nonalcoholic Steatohepatitis Clinical Research Network. Design and validation of a histological scoring system for nonalcoholic fatty liver disease. *Hepatology.* 2005;41:1313–1321.
16. Bedossa P, Poynard T. An algorithm for the grading of activity in chronic hepatitis C. The METAVIR Cooperative Study Group. *Hepatology.* 1996;24:289–293.
17. Terada T, Nakanuma Y. Pathological observations of intrahepatic peribiliary glands in 1,000 consecutive autopsy livers. II. A possible source of cholangiocarcinoma. *Hepatology.* 1990;12:92–97.
18. Terada T, Nakanuma Y. Detection of apoptosis and expression of apoptosis-related proteins during human intrahepatic bile duct development. *Am J Pathol.* 1995;146:67–74.
19. Desmet VJ. Ductal plates in hepatic ductular reactions. Hypothesis and implications. I. Types of ductular reaction reconsidered. *Virchows Arch.* 2011;458:251–259.
20. Desmet VJ. Ductal plates in hepatic ductular reactions. Hypothesis and implications. III. Implications for liver pathology. *Virchows Arch.* 2011;458:271–279.
21. Sato Y, Harada K, Kizawa K, et al. Activation of the MEK5/ERK5 cascade is responsible for biliary dysgenesis in a rat model of Caroli's disease. *Am J Pathol.* 2005;166:49–60.
22. Nakanuma Y, Harada K, Sato Y, et al. Recent progress in the etiopathogenesis of pediatric biliary disease, particularly Caroli's disease with congenital hepatic fibrosis and biliary atresia. *Histol Histopathol.* 2010;25:223–235.
23. Yasoshima M, Sato Y, Furubo S, et al. Matrix proteins of basement membrane of intrahepatic bile ducts are degraded in congenital hepatic fibrosis and Caroli's disease. *J Pathol.* 2009;217:442–451.
24. Raynaud P, Tate J, Callens C, et al. A classification of ductal plate malformations based on distinct pathogenic mechanisms of biliary dysmorphogenesis. *Hepatology.* 2011;53:1959–1966.
25. Saito A, Katayanagi S, Ariizumi T, et al. *Clinical features of cholangiolocellular carcinoma.* Proceeding of Japan Liver Cancer Study Group Meeting, Tokyo. 2011; p. 199.
26. Jarnagin WR, Klimstra DS, Hezel M, et al. Differential cell cycle-regulatory protein expression in biliary tract adenocarcinoma: correlation with anatomic site, pathologic variables, and clinical outcome. *J Clin Oncol.* 2006;24:1152–1160.

Human Pathology (2012) 43, 2177–2186

ELSEVIER

Human PATHOLOGY

www.elsevier.com/locate/humpath

Original contribution

Immunohistochemical characteristics and malignant progression of hepatic cystic neoplasms in comparison with pancreatic counterparts

Takashi Matsubara MD[a,b], Yasunori Sato MD[a], Motoko Sasaki MD[a], Kenichi Harada MD[a], Kazuhiro Nomoto MD[c], Koichi Tsuneyama MD[c], Koichi Nakamura MD[b], Toshifumi Gabata MD[b], Osamu Matsui MD[b], Yasuni Nakanuma MD[a,*]

[a]*Department of Human Pathology, Kanazawa University Graduate School of Medicine, Kanazawa 920-8640, Japan*
[b]*Department of Radiology, Kanazawa University Graduate School of Medicine, Kanazawa 920-8640, Japan*
[c]*Department of Diagnostic Pathology, Graduate School of Medicine and Pharmaceutical Science, University of Toyama, Toyama 930-0194, Japan*

Received 28 November 2011; revised 7 March 2012; accepted 9 March 2012

Keywords:
Biliary tree;
Biliary epithelial cells;
Mucinous cystic neoplasm;
Intraductal papillary neoplasm;
Intraductal papillary mucinous neoplasm

Summary The recent World Health Organization classification for tumors of the digestive system defined grossly and histologically hepatic mucinous cystic neoplasms and intraductal papillary neoplasms of the bile duct separately. In this study, the immunohistochemical features of intraductal papillary neoplasm of the bile duct (19 cases) and hepatic mucinous cystic neoplasm (5 cases) were characterized and compared with those of similar pancreatic lesions, intraductal papillary mucinous neoplasm of the pancreas (12 cases), and pancreatic mucinous cystic neoplasm (6 cases) and with those of other biliary cystic lesions, peribiliary cysts (10 cases). Intraductal papillary neoplasm of the bile duct and intraductal papillary mucinous neoplasm of the pancreas frequently expressed cytokeratin 7; mucin core proteins 1, 2, 5AC, and 6; trypsin; and amylase. Hepatic and pancreatic mucinous cystic neoplasms frequently expressed cytokeratin 7, mucin core proteins 1 and 5AC, estrogen receptor, progesterone receptor, trypsin, and amylase. Estrogen and progesterone receptors were expressed in the subepithelial stromal cells. The groups with intraductal papillary neoplasm of the bile duct and intraductal papillary mucinous neoplasm of the pancreas were different from the groups with hepatic and pancreatic mucinous cystic neoplasm with respect to several phenotypes reflecting gastric and intestinal metaplasia and also the lack of expression of estrogen and progesterone receptors. The Ki-67 and p53 labeling indexes increased significantly with the malignant progression of intraductal papillary neoplasm of the bile duct and intraductal papillary mucinous neoplasm of the pancreas. The p16 labeling index decreased and EZH2 labeling index increased significantly with the malignant progression of intraductal papillary neoplasm of the bile duct and intraductal papillary mucinous neoplasm of the pancreas. In conclusion, intraductal papillary neoplasm of the bile duct and hepatic mucinous cystic neoplasm might be regarded as biliary counterparts of intraductal papillary mucinous neoplasm of the pancreas and pancreatic mucinous cystic neoplasm, respectively, and the mucinous cystic neoplasm and intraductal

* Corresponding author.
E-mail address: pbcpsc@kenroku.kanazawa-u.ac.jp (Y. Nakanuma).

http://dx.doi.org/10.1016/j.humpath.2012.03.007

papillary neoplasm groups differed from each other. Labeling indexes of Ki-67, p53, p16, and EZH2 were comparable in intraductal papillary neoplasm of the bile duct and intraductal papillary mucinous neoplasm of the pancreas along with their malignant progression, suggesting a common carcinogenic process of the tumors.

1. Introduction

The recent World Health Organization classification defined *hepatic mucinous cystic neoplasms* (MCN-Hs) as cyst-forming epithelial neoplasms, usually showing no communication with bile ducts, composed of cuboidal to columnar, mucin-producing epithelium [1]. An association with an ovarian-type subepithelial stroma characterizes MCN-H. A unique biliary tumor named *intraductal papillary neoplasm of the bile duct* (IPNB) has been proposed as another biliary cystic neoplasm [2-6]. IPNB is considered a biliary counterpart of intraductal papillary mucinous neoplasm of the pancreas (IPMN) on the basis of predominant papillary intraductal growth, ductal dilatation, and not-infrequent overproduction of mucin, as well as, frequently, communication with the neighboring bile duct lumen [2-6]. These 2 types of cystic neoplasm need to be distinguished from other cystic liver lesions including simple cysts and peribiliary cysts (PB cysts) [1,7].

Polycomb group proteins are epigenetic chromatin modifiers involved in cancer development. Polycomb group proteins exist in at least 2 separate complexes, polycomb repressive complex (PRC)2 and PRC1 [8-10]. Bmi1 and EZH2 are representative of PRC1 and PRC2, respectively. Recent studies showed that EZH2 is a chromatin-modifying enzyme and interacts with key elements that control cell growth and proliferation such as the genes *Rb* and $p16^{INK4a}$ [9,10]. p16 and EZH2 are reportedly involved in the progression from biliary intraepithelial neoplasia (BilIN), a premalignant or early neoplastic biliary lesion, to invasive cholangiocarcinoma [8]. Cell proliferative activity and the aberrant expression of p53 are known to increase with the progression of BilIN and also IPNB [9,10]. IPNB and MCN-H are also known as preneoplastic and early neoplastic lesions followed by invasive cholangiocarcinoma (tubular adenocarcinoma and mucinous carcinoma) [1,2,11]. However, the exact molecular and genetic mechanisms associated with the malignant progression of IPNB and MCN-H with respect to pancreatic counterparts remain unexplored.

Recent pathologic studies suggested that IPNB and MCN-H correspond to IPMN and MCN of the pancreas (MCN-P), respectively [5]. IPMN and MCN-P are known to progress to invasive carcinoma of the pancreas. However, an exact comparison of these pancreatic and biliary neoplasms with respect to immunophenotypes and malignant progression has yet to be undertaken.

In this study, the immunohistochemical characteristics of IPNB and MCN-H were compared with those of pancreatic counterparts and PB cysts. The mechanisms behind the progression of IPNB and MCN-H with respect to cell kinetics, p53, EZH2, and p16 were also compared with those for pancreatic counterparts, IPMN and MCN-P, by using surgically resected specimens.

2. Materials and methods

2.1. Case selection

A total of 19 cases of IPNB, 5 cases of MCN-H, 10 cases of PB cysts, 12 cases of IPMN, and 6 cases of MCN-P were collected from the Department of Human Pathology, Kanazawa University Graduate School of Medicine; the Pathologic Diagnostic Service, Kanazawa University Hospital; and affiliated hospitals (1993-2011). All except 3 autopsy specimens of PB cysts were surgically resected. The pathologic diagnosis of these diseases and also the histologic grading of IPNB, MCN-H, PB cysts, IPMN, and MCN-P were performed according to the recent World Health Organization classification of tumors of the digestive system [1,3]. In this study, the hilar bile ducts and intrahepatic large bile ducts are collectively referred to as *large bile ducts*.

Clinical and pathologic features of the cases are listed in Tables 1, 2, and 3. All patients examined were adults, and all patients with MCN-H and MCN-P were female (Table 1). All MCN-Ps were located in the pancreatic tail, and all MCN-Hs in the left medial segment (Table 2). IPNB

Table 1 Clinical features of the cases examined

Lesions	No. of cases	Sex (male/female)	Average age (y) (range)
IPNB	19	11/8	64.3 (38-80)
MCN-H	5	0/5	58.0 (40-66)
PB cysts	10	7/3	67.1 (52-83)
IPMN	12	9/3	70.3 (57-80)
MCN-P	6	0/6	50.2 (27-81)

Table 2 Pathologic features of the cystic neoplasms of the liver and pancreas

Pathologic features	IPNB (n = 12)[a]	MCN-H (n = 5)	IPMN (n = 12)	MCN-P (n = 6)
Size (mm), mean (range)	50.3 (15-110)	100 (35-140)	41.1 (20-90)	61.2 (25-98)
Main location				
Liver				
Left lateral segment	4 (33%)	0 (0%)		
Left medial segment	6 (50%)	5 (100%)		
Right robe	2 (17%)	0 (0%)		
Pancreas				
Head			2 (17%)	0 (0%)
Body			3 (25%)	0 (0%)
Tail			7 (58%)	6 (100%)
Multiple lesions	0 (0%)	0 (0%)	2 (17%)	0 (0%)

[a] Among the 19 cases of IPNB examined, 12 corresponded to cystic variant of IPNB, and the results of these 12 cases are shown. n, number of cases.

predominantly affected the left segments, and IPMN was in the body and tail. The degree of atypia and incidence of invasion of IPNB, MCN-H, IPMN, and MCN-P are shown in Table 3. Most MCN-H and MCN-P cases involved low-grade intraepithelial neoplasia/dysplasia, whereas half of the IPNB cases involved high-grade intraepithelial neoplasia and were associated with an invasive carcinoma. About half of the IPMN cases were also associated with an invasive carcinoma. These results were compatible with other reports on MCN-H and MCN-P and on IPNB and IPMN [1,3,5].

2.2. Tissue preparation

Tissue specimens were fixed in 10% neutral-buffered formalin and embedded in paraffin. More than 20 consecutive 4-μm-thick sections were cut from each paraffin block, and some of them were stained with hematoxylin and eosin and Azan-Mallory stain for the identification of the arterial architecture of the bile duct and characterization of biliary epithelial lesions. The remaining sections were used for immunohistochemistry.

2.3. Immunostaining

Immunostaining was performed using formalin-fixed, paraffin-embedded tissue sections in all cases of hepatic and pancreatic cystic disease. The antibodies and their sources, optimal dilutions, and antigen retrieval are shown in Table 4. Briefly, after the blocking of endogenous peroxidase activity, deparaffinized and hydrated sections were incubated in a protein block solution (DakoCytomation, Glostrup, Denmark). The sections were incubated overnight at 4°C with primary antibodies against cytokeratin (CK)7, CK20, mucin core protein (MUC)1, MUC2, MUC5AC, MUC6, estrogen receptor (ER), progesterone receptor (PgR), p53, Ki-67, EZH2, and p16. The sections were then treated with secondary antibodies conjugated to a peroxidase-labeled polymer, the EnVision system (DakoCytomation). Color development was performed using 3,3'-diaminobenzidine tetrahydrochloride (DAB) or Tyramide Signal Amplification Plus Fluorescence (Tyramide Signal Amplification PLUS Fluorescein/TMR Kits; PerkinElmer, Waltham, MA), and the sections were counterstained with hematoxylin or methyl green. Negative controls were carried out by substitution of the primary antibodies with nonimmunized serum.

2.4. Semiquantitative evaluation

The results of the immunohistochemical staining of CK7, CK20, MUC1, MUC2, MUC5AC, and MUC6 were graded into 4 categories based on the percentage of positive cells among neoplastic or hyperplastic epithelial cells (CK7, CK20, MUC1, MUC2, MUC5AC, and MUC6) and of positive nuclei in subepithelial stromal cells (ER and PgR) in individual cases: little or no staining (−), weak (+), moderate (++), and strong (+++). The proportion of cells positive for these proteins was less than 5% in (−) in individual lesions, ranged from 5% to 20% in (+) and from 20% to 50% in (++), and was more than 51% in (+++).

Table 3 Histologic grade and phenotype of the cases examined

Grade	IPNB	MCN-H	IPMN	MCN-P
Low-grade intraepithelial neoplasia/dysplasia	1 (5%)	3 (60%)	0 (0%)	5 (83%)
Intermediate-grade intraepithelial neoplasia/dysplasia	7 (37%)	0 (0%)	5 (42%)	0 (0%)
High-grade intraepithelial neoplasia/dysplasia	6 (32%)	1 (20%)	2 (17%)	0 (0%)
Associated with invasive carcinoma	5 (26%)	1 (20%)	5 (42%)	1 (17%)

Table 4 Primary antibodies used in this study

Primary antibody	Clone	Animal	Mono or poly	Dilution	Source
CK7	OV-TL 12/30	Mouse	Mono	1:50	DakoCytomation
CK20	K_s 20.8	Mouse	Mono	1:50	DakoCytomation
MUC1	DF3	Mouse	Mono	1:50	TFB, Tokyo, Japan
MUC2	Ccp58	Mouse	Mono	1:100	Novocastra, Newcastle, UK
MUC5AC	CLH2	Mouse	Mono	1:200	Novocastra
MUC6	CLH5	Mouse	Mono	1:200	Novocastra
ER	6F11	Mouse	Mono	1:100	Novocastra
PgR	312	Mouse	Mono	1:40	Novocastra
Pancreatic trypsin	–	Mouse	Mono	1:1500	Chemicon, Billerica, MA
Pancreatic amylase	1855 EE7	Mouse	Mono	1:1 (prediluted)	Innovex Bioscience, Richmond, CA
P53	DO-7	Mouse	Mono	1:100	DakoCytomation
Ki-67	MIB-1	Mouse	Mono	1:200	DakoCytomation
EZH2	11	Mouse	Mono	1:100	Transduction, San Jose, CA
P16	JC2	Mouse	Mono	1:100	Neomarkers, Freemont, CA

Mono, monoclonal antibodies; poly, polyclonal antibodies. –, the clone name is unavailable.

2.5. Labeling index

The immunohistochemical expression of p53, Ki-67, EZH2, and p16 was evaluated in 5 to 10 randomly selected higher-power fields of the section in each case, in which more than 500 nuclei of the epithelial cells were included. The percentage of the positively stained cells is expressed as a labeling index (LI).

2.6. Statistical analysis

Numerical data are presented as mean ± SD. Data from different groups were compared using a 1-way analysis of variance and examined with the Kruskal-Wallis test. The results were considered significant if the P value was less than .05.

3. Results

3.1. Immunophenotypes

Typical immunohistochemical expression patterns of CKs, MUCs, ER, PgR, amylase, and trypsin are shown in Fig. 1. CK7 (Fig. 1A) and CK20 (Fig. 1B) were expressed in the cytoplasm of neoplastic epithelial cells in cases of IPNB. MUC1 (Fig. 1C), MUC2 (Fig. 1D), MUC5AC (Fig. 1E), and MUC6 (Fig. 1F) were expressed in the cytoplasm and also on the luminal surface of neoplastic epithelial cells in cases of IPNB. Amylase (Fig. 1G) and trypsin (Fig. 1H) were expressed in the cytoplasm of neoplastic epithelial cells of IPNB. ER (Fig. 1I) and PgR (Fig. 1J) were expressed in the mesenchymal stromal cells beneath the epithelium in cases of MCN-H.

The results of the semiquantitative evaluation of the immunohistochemistry in cases of IPNB, MCN-H, PB cysts, IPMN, and MCN-P are shown in Fig. 2.

3.1.1. Expression of CKs

CK7, a biliary CK, was frequently and extensively expressed in almost all cases examined irrespective of the type of disease. CK20, an intestinal CK, was infrequently expressed in IPNB, PB cysts, IPMN-P, and MCN-P, which might reflect the intestinal metaplasia of neoplastic cells.

3.1.2. Expression of MUCs

MUC1 was expressed similarly in about 40% of IPNB and MCN-H cases and also in about half of IPMN and MCN-P cases, whereas MUC1 was not expressed in PB cysts. MUC2, an intestinal mucin, was expressed in about half of IPNB and IPMN, but not in MCN-H, MCN-P, and PB cysts. MUC5AC, a gastric foveolar mucin, was frequently observed in IPNB and IPMN groups; in MCN-H and MCN-P groups, the degree and frequency of its expression were relatively low. MUC5AC was not expressed in PB cysts. MUC6, a gastric pyloric gland mucin, was frequently expressed in IPNB and IPMN. Its expression was also higher in MCN-P and PB cysts, but relatively low and focal in MCN-H.

3.1.3. Expression of ER and PgR

PgR was expressed in subepithelial stromal cells in all cases of MNC-H and MCN-P, and ER was also expressed in subepithelial stromal cells in all cases except for 1 hepatic MNC-H case. Interestingly, PgR and ER were negative in IPNB, IPMN, and PB cysts.

3.1.4. Expression of amylase and trypsin

Amylase was similarly expressed in 40% to 50% of the cases of IPNB, IPMN, MCN-H, and MCN-P. Its expression in PB cysts was less frequent (about 20%) and focal. Trypsin was expressed in about 40% of IPNB and MCN-H and more frequently in IPMN and MCN-P, whereas its expression in PB cysts was relatively low and focal.

The characteristic features of the immunophenotypes of IPNB, MCN-H, PB cysts, IPMN, and MCN-P are summarized in Table 5. MCN-H and MCN-P shared many

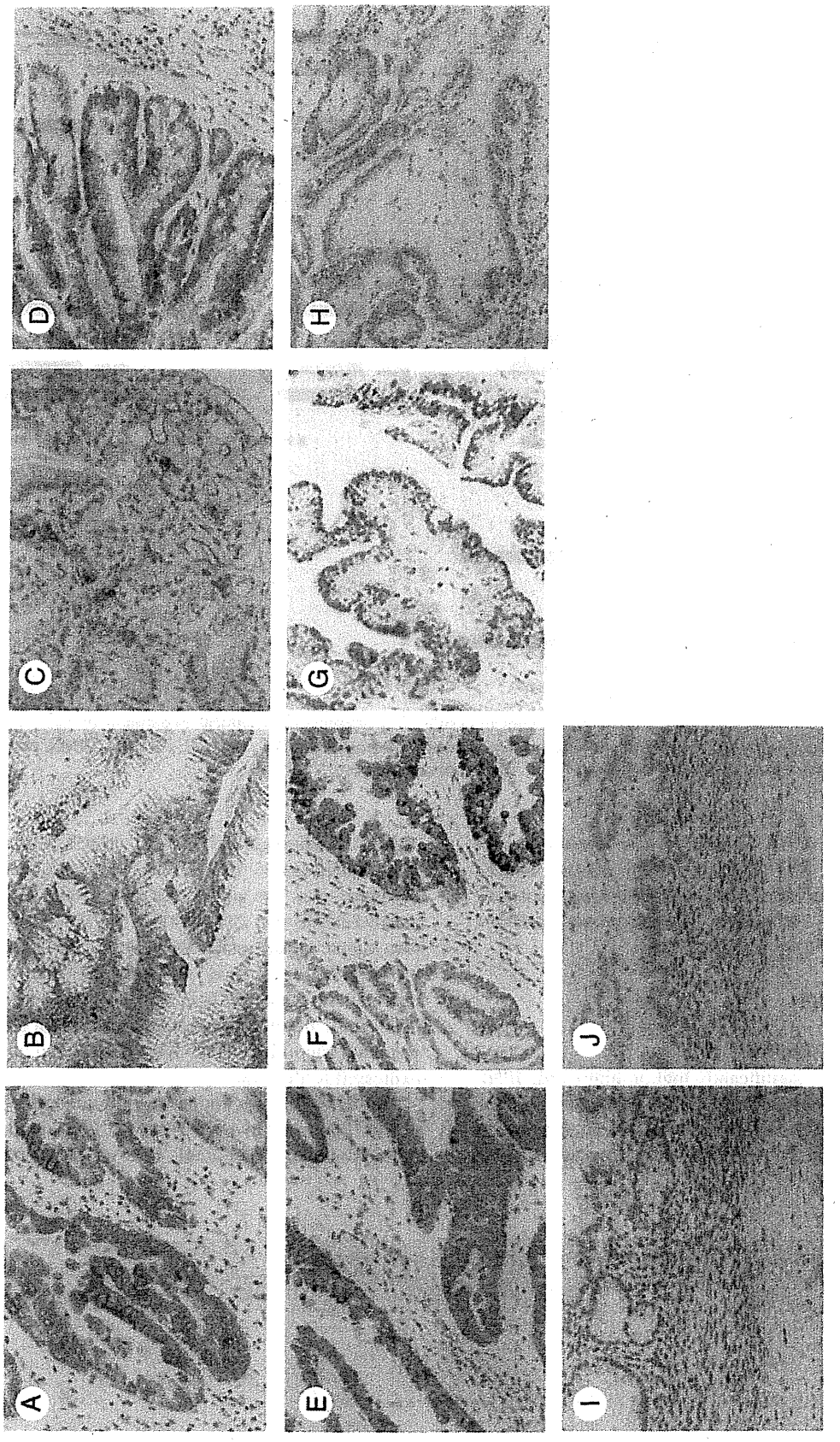

Fig. 1 Representative immunophenotypes of IPNB and MCN-H. Immunohistochemical expression of CK7 (A), CK20 (B), MUC1 (C), MUC2 (D), MUC5AC (E), MUC5AC (F), amylase (G), and trypsin (H) was observed in neoplastic epithelial cells of IPNB. ER (I) and PgR (J) were expressed in the mesenchymal stromal cells beneath the epithelium of MCN-H.

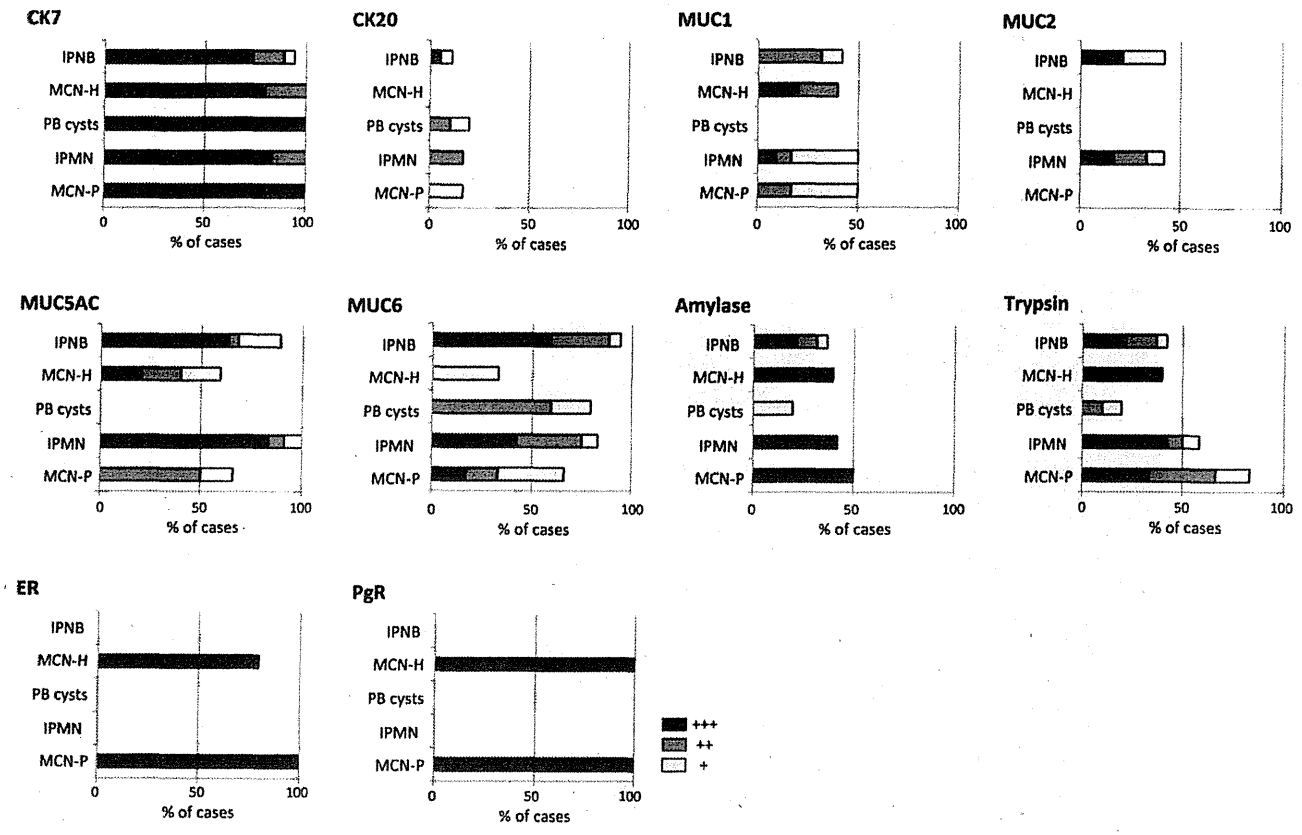

Fig. 2 Semiquantitative analysis of the immunohistochemical results. The immunohistochemical expression of CK7, CK20, MUC1, MUC2, MUC5AC, MUC6, amylase, trypsin, ER, and PgR was evaluated for the cases of IPNB, MCN-H, PB cysts, IPMN, and MCN-P. The semiquantitative analysis was performed as described in the "Materials and Methods."

immunophenotypes. IPNB and IPMN also showed similar immunophenotypes. The IPN and MCN groups showed different immunophenotypes such as the expression status of MUC2, PgR, and ER. In contrast, PB cysts showed different immunophenotypes from these 2 groups.

3.2. Labeling index

3.2.1. LI for Ki-67 and p53

The Ki-67 LI was significantly high in high-grade IPNB (11.29 ± 8.89 in 17 foci) and in invasive IPNB (20.9 ± 4.01 in 3 foci) compared with that in low- to intermediate-grade IPNB (3.02 ± 3.52 in 17 foci) (Fig. 3A). The p53 LI was higher in high-grade IPNB (8.76 ± 10.55) than in low- to intermediate-grade IPNB (2.41 ± 3.50), although the difference was not significant (Fig. 3A). The p53 LI in invasive IPNB was 2.09 ± 4.01. The Ki-67 LI and p53 LI were higher in high-grade MCN-H (12.5 ± 0.42 in 2 foci and 8.1 ± 6.08 in 2 foci, respectively) than in low- to intermediate-grade MCN-H (3.16 ± 4.57 in 5 foci and 0.34 ± 0.61 in 5 foci, respectively), although the differences were not significant (Fig. 3A). Ki-67 and p53 were not expressed in PB cysts.

The Ki-67 LI was higher in high-grade IPMN (13.46 ± 7.41 in 7 foci) and invasive IPMN (9.57 ± 2.68 in 3 foci) than in low- to intermediate-grade IPMN (3.19 ± 3.05 in 11 foci)

Table 5 Summary of immunophenotypes of the cystic lesions of the liver and pancreas

Lesions	CK7	CK20	MUC1	MUC2	MUC5AC	MUC6	ER	PgR	Trypsin	Amylase
IPNB	+++	+	++	++	+++	+++	−	−	++	++
MCN-H	+++	−	++	−	+++	++	+++	+++	++	++
PB cysts	+++	+	−	−	−	+++	−	−	+	+
IPMN	+++	+	++	++	+++	+++	−	−	+++	++
MCN-P	+++	+	++	−	+++	+++	+++	+++	+++	++

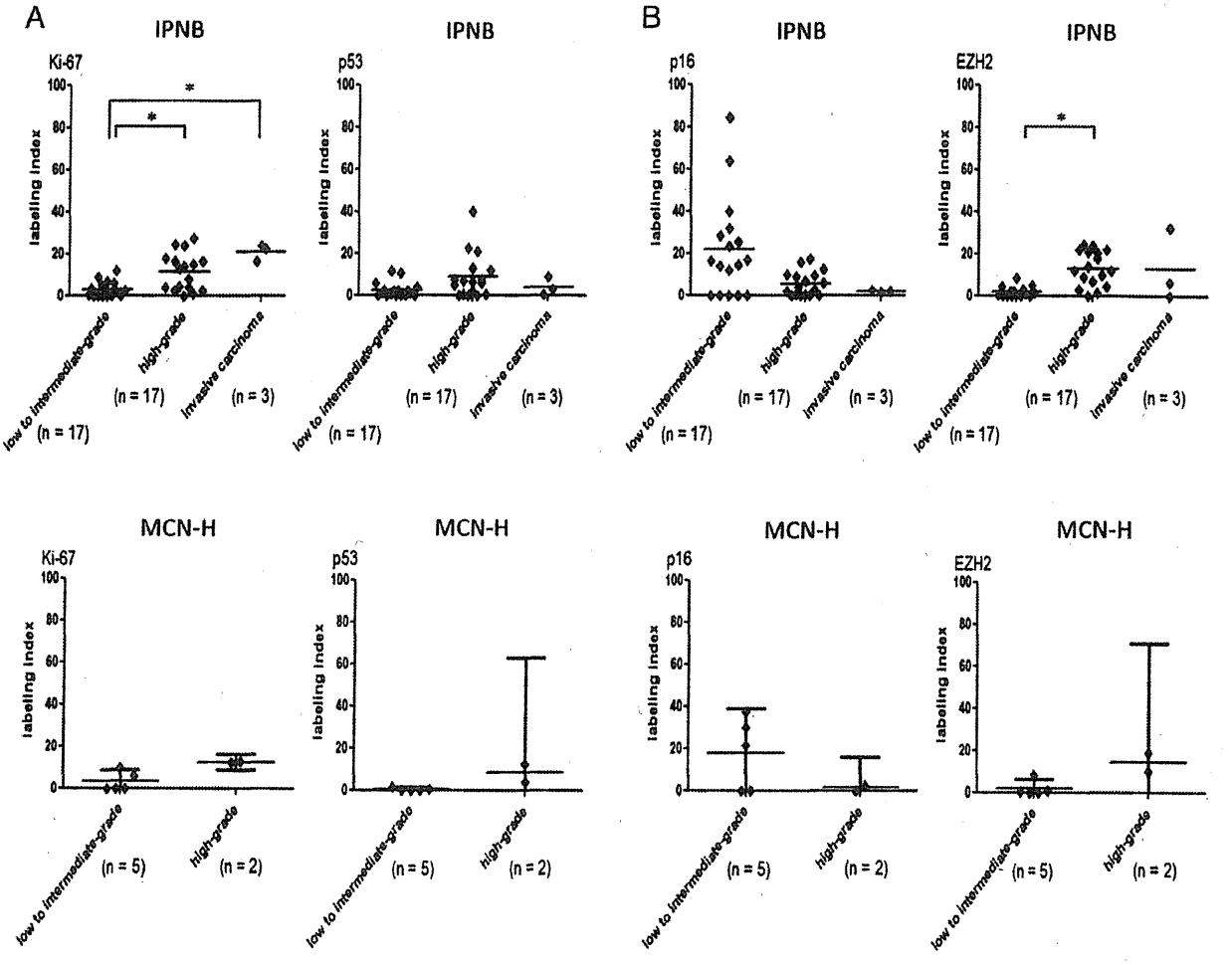

Fig. 3 LI of Ki-67, p53, p16, and EZH2 in IPNB and MCN-H. A, The Ki-67 LI was significantly higher in high-grade IPNB and invasive parts of IPNB than in low- to intermediate-grade IPNB. The p53 LI showed a similar tendency but the difference was not statistically significant. The Ki-67 LI and p53 LI were slightly higher in high-grade MCN-H than in low- to moderate-grade MCN-M. B, The EZH2 LI was higher in high-grade IPNB and invasive parts of IPNB than in low- to intermediate-grade IPNB, and a significant difference was observed between the groups of high-grade IPNB and low- to intermediate-grade IPNB. The p16 LI tended to be low in high-grade IPNB and invasive IPNB. The p16 LI was relatively high in low-grade MCN-Hs, and the EZH2 LI was relatively high in high-grade MCN-Hs, although there was no statistically significant difference. $^{*}P < .05$.

(Fig. 4A). The difference in the former was statistically significant, whereas that in the latter was not. The p53 LI was higher in high-grade IPMN (28.37 ± 35.22) than in low- to intermediate-grade IPMN (1.29 ± 2.39) (Fig. 4A). The p53 LI in invasive IPMN was 26.87 ± 40.93. The Ki-67 LI tended to be high in high-grade MCN-P and invasive MCN-P (19.8 and 21.0, respectively) compared with that in low- to moderate-grade MCN-P (2.12 ± 2.18) (Fig. 4A). The p53 LIs in low- to intermediate-grade MCN-P, high-grade MCN-P, and invasive MCN-P were 0.1 ± 0.24, 1.2, and 1.3, respectively (Fig. 4A).

3.2.2. LI for p16 and EZH2

The p16 LI tended to be low in high-grade IPNB (5.56 ± 5.75 in 17 foci) compared with that in low- to intermediate-grade IPNB (21.75 ± 23.49 in 17 foci), although the difference was not significant (Fig. 3B). The p16 LI in invasive IPNB was 1.7 ± 0.53 in 3 foci. The EZH2 LI was significantly high in high-grade IPNB (13.05 ± 8.26) compared with that in low- to intermediate-grade IPNB (1.69 ± 2.21) (Fig. 3B). The EZH2 LI in invasive IPNB was 12.93 ± 17.08. The p16 LI was similar in low- to intermediate-grade MCN-H (17.76 ± 17.17 in 5 foci) and in high-grade MCN-H (1.15 ± 1.63 in 2 foci) (Fig. 3B). The EZH2 LI tended to be high in high-grade MCN-H (14.25 ± 6.29) compared with that in low- to moderate-grade MCN-H (1.78 ± 3.60) (Fig. 3B). P16 and EZH2 were not expressed in PB cysts.

The p16 LI was higher in low- to intermediate-grade IPMN (37.09 ± 26.28 in 11 foci) than in high-grade IPMN (4.69 ± 3.45 in 7 foci), although the difference was not significant (Fig. 4B). The p16 LI in invasive

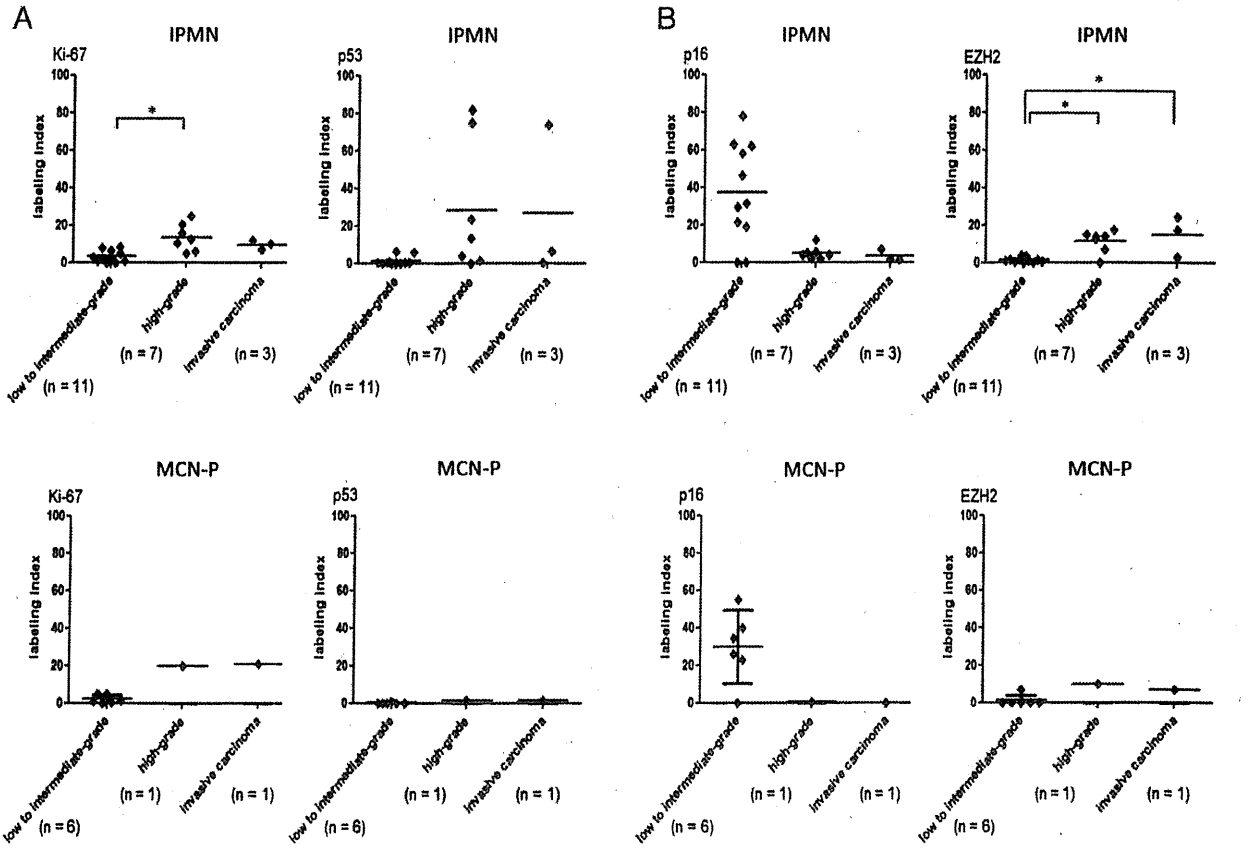

Fig. 4 LI of Ki-67, p53, p16, and EZH2 in IPMN and MCN-P. A, The Ki-67 LI was higher in high-grade IPMN and invasive parts of IPMN than in low- to moderate-grade IPMN. It was also relatively high in high-grade and invasive MCN-P, although the difference was not significant. The p53 LI tended to be high in high-grade IPMN and invasive IPMN. p53 was not expressed in MCN-P irrespective of grade. B, The EZH2 LI was significantly higher in high-grade IPMN and invasive parts of IPMN than in low- to intermediate-grade IPMN. The p16 LI was relatively low in high-grade and invasive IPMN compared with that in low- to intermediate-grade IPMN. The p16 LI was relatively high in low- to intermediate-grade MCN-P in comparison with that in high-grade MCN-P and invasive MCN-P, although there was no statistically significant difference (B). $*P < .05$.

IPMN was 3.13 ± 3.00 in 3 foci. The EZH2 LI was significantly higher in high-grade IPMN and invasive IPMN (11.37 ± 5.94 and 14.87 ± 10.99, respectively) than in low- to moderate-grade IPMN (1.22 ± 1.33) (Fig. 4B). The p16 LI was higher in low- to intermediate-grade MCN-P (29.71 ± 18.48 in 6 foci) than in high-grade MCN-P and in invasive MCN-P (0.4 and 0.0, respectively, in a single focus), although the difference was not significant (Fig. 4B). The EZH2 LI was low in each group of low- to intermediate-grade, high-grade, and invasive MCN-P (Fig. 4B).

4. Discussion

There have been several reports on radiologic and histologic studies concerning similarities between IPNB and IPMN and also between MCN-H and MCN-P [2,6,7]. This study additionally revealed that there were immunophenotypic similarities between IPNB and IPMN and between MCN-H and MCN-P, and also some differences between the MCN group (MCN-H and MCN-P) and IPN group (IPNB and IPMN). The MCN group differed from the IPN group with respect to the expression of ER and PgR, owing to the presence of a subepithelial ovarian-like stroma in the former. In accordance with MUC2 expression, CK20 expression was relatively frequent in the IPN group in comparison with that in the MCN group. MUC2 and CK20 expressions are regarded as an intestinal phenotype. Furthermore, MUC5AC and MUC6 were relatively more frequent in the IPN group than in the MCN group. MUC5AC and MUC6 are gastric foveolar and pyloric gland markers, respectively [12]. These results suggest frequent intestinal and gastric metaplasia in the IPN group in comparison with that in the MCN group [4]. These findings also support the hypothesis that

IPMN-P is a pancreatic counterpart of IPNB, and MCN-P is that of MCN-H, and that the IPN and MCN groups seem to undergo different processes of tumorigenesis.

It is generally thought that IPNB and also MCN-H eventually develop into invasive cholangiocarcinomas (ordinary tubular adenocarcinomas as well as mucinous carcinomas), although the exact molecular and genetic mechanisms involved remain unexplored. It was found in this study that the Ki-67 and p53 LIs increased significantly with the progression from low- to intermediate-grade IPNB to high-grade and invasive IPNB. A similar tendency was also noted in MCN-Hs. The p16 LI decreased and EZH2 LI increased significantly with the progression from low- to intermediate-grade IPNB to high-grade and invasive IPNB. In the progression of BilIN, another preneoplastic biliary lesion followed by invasive cholangiocarcinoma, increased Ki-67 LI and increased EZH2 LI with decreased p16 LI were pointed out [8]. Therefore, it seems conceivable that IPNB and BilIN share malignant progression along the biliary tree, although why cystic and papillary changes and mucus hypersecretion were predominant in the former remains unclear.

Interestingly, the expression of Ki-67 and p53 and that of p16 and EZH2 found in IPNB were similarly found in IPMN, suggesting that IPNB and IPMN have similar or the same malignant progression. Recently, Nakahara et al [13] also reported a role for the overexpression of EZH2 in the progression of IPMN. These results support the suggestion of similarities between IPNB and IPMN. MCN-H and MCN-P also showed similar tendencies in terms of the expression of Ki-67 and p53 and that of p16 and EZH2. However, the number of MCN cases was too small to speculate on the malignant progression in the MCN group.

There are other hepatic cystic lesions that are different from MCN-H and IPNB. In particular, PB cysts, which are a benign multicystic lesion derived from peribiliary glands and usually found in the hepatic hilar and perihilar areas, should be differentiated from MCH-H and IPNB [3,4,13]. To date, there have been no comparative immunohistochemical studies of PB cysts and MCN-H and IPNB. It was found in this study that expression patterns of MUC1, MUC2, and MUC5AC and, to a lesser degree, trypsin and amylase were different between PB cysts and others (MCN-H and IPNB), although some phenotypes such as CK7 were found frequently in both. PgR and ER were absent in PB cysts. Furthermore, PB cysts failed to show proliferative activities such as an increased Ki-67 index and to express p53, p16, and EZH2, suggesting that they have no neoplastic features and no tendency to undergo malignant transformation. Taking these findings together, PB cysts are different from MCN-H and IPNB with respect to immunophenotypes and also biological activities in addition to histologic features.

In conclusion, the findings of this study suggest that IPNB and MCN-H are biliary counterparts of IPMN and MCN-P, respectively, with respect to their immunophenotypes. The MCN group was shown to be different from the IPN group with respect to several immunophenotypes, reflecting frequent intestinal and gastric metaplasia in the latter and the constant expression of PgR and ER in subepithelial stromal cells in the former. IPNB and MCN-H differed from PB cysts immunohistochemically. The Ki-67 and p53 LIs increased significantly with the progression of IPNB and IPMN. The p16 LI decreased and EZH2 LI increased significantly with the progression of IPNB and IPMN, respectively, suggesting a common carcinogenic process in these preneoplastic/early neoplastic lesions of the biliary tree and pancreas.

Acknowledgments

The authors thank Dr Shin Ishiyama and Dr Akio Uchiyama (Department of Human Pathology, Toyama Prefectural Central Hospital, Toyama, Japan) and Dr Tetsuo Ohta and Dr Hirohisa Kitagawa (Department of Gastroenterological Surgery, Kanazawa University Graduate School of Medicine, Kanazawa, Japan) for providing tissue samples.

References

[1] Tsui WMS, Adsay NV, Crawford JM, et al. Mucinous cystic neoplasm of the liver. In: Bosman FT, Carneiro F, Hruban RH, Theise ND, editors. WHO classification of tumours of the digestive system; World Health Organization of Tumours, 4th ed. Lyon: IARC; 2010. p. 236-40.

[2] Chen TC, Nakanuma Y, Zen Y, et al. Intraductal papillary neoplasia of the liver associated with hepatolithiasis. Hepatology 2001;34: 651-8.

[3] Nakanuma Y, Curabo MP, Franceschi S, et al. Intrahepatic cholangiocarcinoma. In: Bosman FT, Carneiro F, Hruban RH, Theise ND, editors. WHO classification of tumours of the digestive system; World Health Organization of Tumours, 4th ed. Lyon: IARC; 2010. p. 217-24.

[4] Zen Y, Fujii T, Itatsu K, et al. Biliary papillary tumors share pathological features with intraductal papillary mucinous neoplasm of the pancreas. Hepatology 2006;44:1333-43.

[5] Zen Y, Pedica F, Patcha VR, et al. Mucinous cystic neoplasms of the liver: a clinicopathological study and comparison with intraductal papillary neoplasms of the bile duct. Mod Pathol 2011;24:1079-89.

[6] Lim JH, Zen Y, Jang KT, Kim YK, Nakanuma Y. Cyst-forming intraductal papillary neoplasm of the bile ducts: description of imaging and pathologic aspects. AJR Am J Roentgenol 2011;197: 1111-20.

[7] Kida T, Nakanuma Y, Terada T. Cystic dilatation of peribiliary glands in livers with adult polycystic disease and livers with solitary nonparasitic cysts: an autopsy study. Hepatology 1992;16: 334-40.

[8] Sasaki M, Yamaguchi J, Itatsu K, Ikeda H, Nakanuma Y. Overexpression of polycomb group protein EZH2 relates to decreased expression of p16 INK4a in cholangiocarcinogenesis in hepatolithiasis. J Pathol 2008;215:175-83.

[9] Valk-Lingbeek ME, Bruggeman SW, van Lohuizen M. Stem cells and cancer; the polycomb connection. Cell 2004;118:409-18.